

PIOTR BOGUSZ, MARIUSZ KORKOSZ, JAN PROKOP*

ANALYSIS OF THE INFLUENCE OF WINDING CONFIGURATION ON THE PROPERTIES OF A SWITCHED RELUCTANCE MOTOR

ANALIZA WPŁYWU KONFIGURACJI UZWOJEŃ BIEGUNÓW NA WŁAŚCIWOŚCI SILNIKA RELUKTANCYJNEGO PRZEŁĄCZALNEGO

Abstract

In this paper, the series configuration of pole winding connections in each phase of a three-phase 12/8 switched reluctance motor was analyzed. Based on the simulation model, the effect of magnetic couplings on motor properties was determined. Static characteristics were obtained for NNSS and NSNS configurations. Voltage, current, and electromagnetic torque waveforms were determined. Simulation results were verified through laboratory tests.

Keywords: switched reluctance motor, three-phase motor, winding pole configurations

Streszczenie

W niniejszym artykule analizowano konfigurację szeregową uzwojeń biegunów każdego pasma trójfazowego silnika reluktancyjnego przełączalnego 12/8. Na podstawie modelu symulacyjnego określono wpływ sprzężeń magnetycznych na właściwości silnika. Dla konfiguracji NNSS i SNS zostały wyznaczone charakterystyki statyczne. Wyznaczono też przebiegi czasowe napięć, prądów oraz momentu elektromagnetycznego. Dokonano weryfikacji laboratoryjnej.

Słowa kluczowe: silnik reluktancyjny przełączalny, silnik trójfazowy, konfiguracja uzwojeń biegunów

DOI: 10.4467/2353737XCT.15.035.3835

* Ph.D. Eng. Piotr Bogusz, D.Sc. Ph.D. Eng. Mariusz Korkosz, D.Sc. Ph.D. Eng. Jan Prokop, Faculty of Electrical and Computer Engineering, Rzeszów University of Technology, Poland.

1. Introduction

With increasing the number of poles per phase in a switched reluctance motor (SRM), the number of possible configurations of the connection of winding poles also increases. In the standard version of the switched reluctance machine, two pole winding configurations, (serial and parallel) are possible [1]. At the same time, the presence of a higher number of poles per phase and a higher number of phases results in the multiplication of the number of possible ways of particular pole windings supply [2–5].

The purpose of the paper is to present the results of the analysis on the influence of configuration on poles windings connected in series in a 12/8 switched reluctance motor on its static properties and current waveforms.

With the serial connection, there are two basic configurations possible for each of the phases, NNSS and NSNS. For each of these phase configurations, a number of variants is available in which individual pole windings can be supplied. For selected pole winding supply configuration, simulations were carried out aimed at the evaluation of the effect of magnetic couplings between individual motor phases from which voltage, current, and electromagnetic torque waveforms were determined. In laboratory conditions, current and voltage waveforms were registered under specific motor supplying conditions for a selected pole winding supplying configuration. Finally, example mechanical characteristics of the motor were determined.

2. Motor parameters and poles windings configuration

A physical model of the switched reluctance motor was developed in the course of an earlier research project [6]. It allows the obtaining of any configuration of windings. Table 1 summarizes selected parameters of the motor prototype constituting the subject of the tests.

Table 1

Selected parameters of the examined motor

Number of phases	3
Number of stator poles	12
Number of rotor poles	8
Rated power	1 kW
Rated voltage	300 V
Rated speed	30 000 rpm
Magnetic material	M470-50A

Assuming that pole windings of each phase in a 12/8-pole three-phase SRM are connected in series, two basic configurations of pole windings can be distinguished, NNSS and NSNS. Figure 1 shows both pole winding supply configurations considered here in the basic version of types NNNNNSSSSSS (Fig. 1a)) and NNNSSNNSSSS (Fig. 1c)). Additionally, Figs.

1b) and d) depict configurations in which input terminals of individual phases are shifted with respect to each other, i.e. configurations NSSNNSNNSN and NSNSNSNSNSNS, respectively. The phase denoted as *Ph1* comprises poles A1–A4, while phases *Ph2* and *Ph3* include poles B1–B4 and C1–C4, respectively.

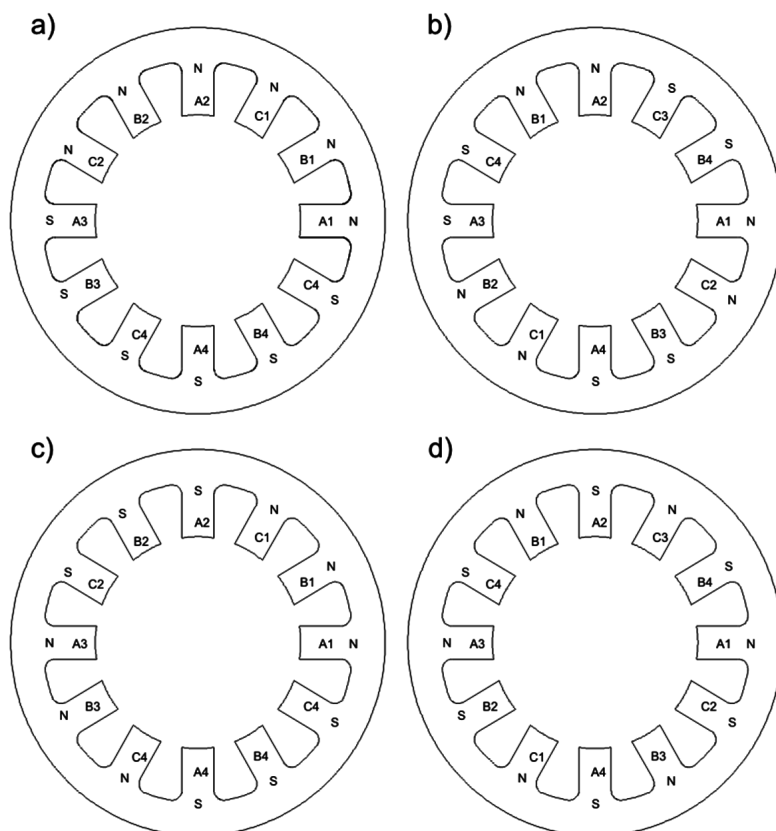


Fig. 1. The considered pole winding supplying configurations in the three-phase 12/8-pole SRM

3. Simulations – determination of static characteristics

The numerical model of the SRM has been developed in a computer program based on the finite element method [7]. Figure 2 presents plots of electromagnetic torque average value T_{eav} as a function of current I in one of the motor phases for the analyzed winding supplying configurations, i.e. NNSS and NSNS.

The analyzed configurations (NNSS, NSNS) don't have much effect on the produced electromagnetic torque value in the motor design considered herein. The main flux ψ_{11} determined as a function of the rotor position θ is shown in Fig. 3, while the coupled fluxes ψ_{12} and ψ_{13} are plotted in Figs. 4 and 5, respectively.

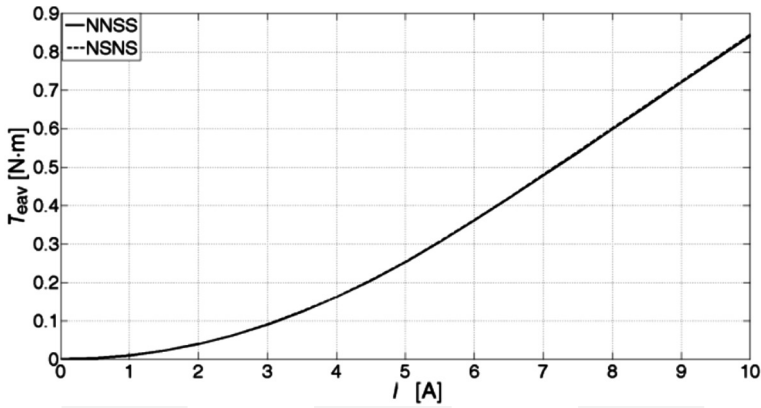


Fig. 2. The electromagnetic torque T_{eav} as a function of rotor position θ at $I = \text{var}$ for configurations NNSS and NSNS

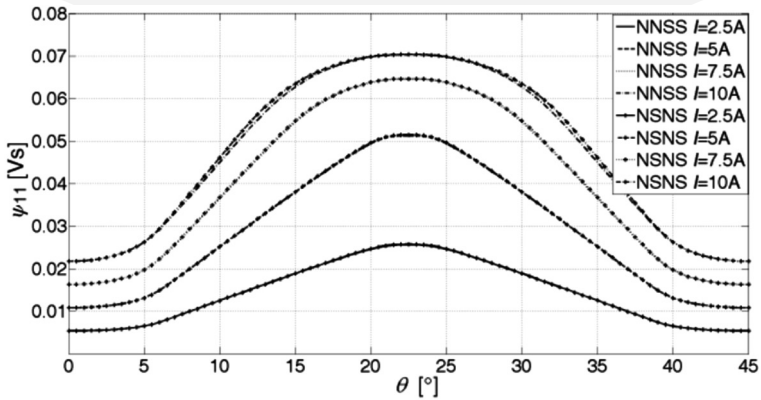


Fig. 3. The main flux ψ_{11} as a function of rotor position θ at $I = \text{var}$ for configurations NNSS and NSNS

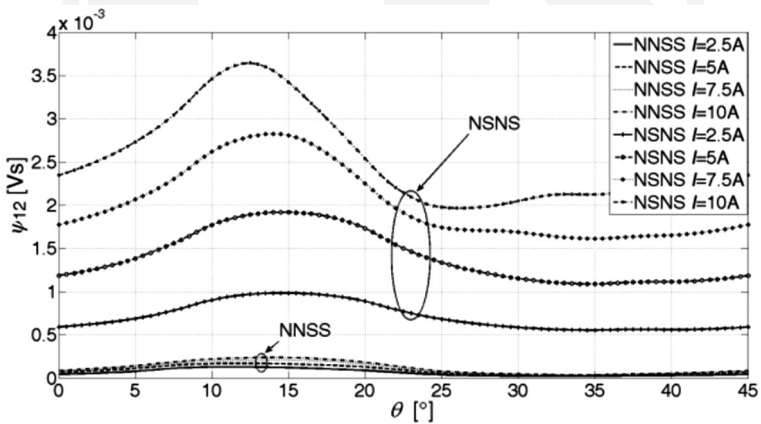


Fig. 4. The main flux ψ_{12} as a function of rotor position θ at $I = \text{var}$ for configurations NNSS and NSNS

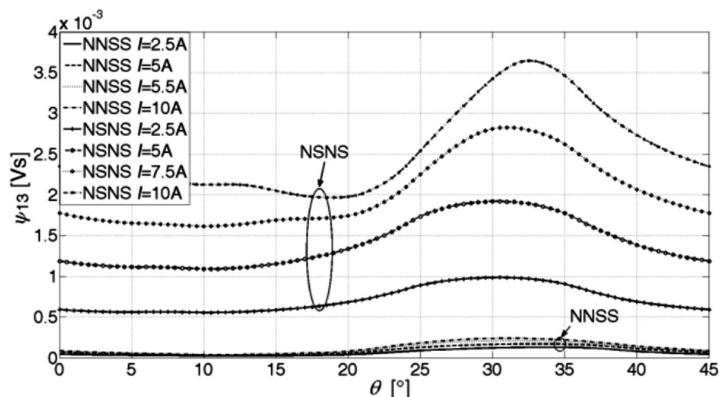


Fig. 5. The coupled flux ψ_{13} as a function of rotor position θ at $I = \text{var}$ for configurations NNSS and NSNS

The main flux ψ_{11} depends only in a small degree on the pole winding configuration type. In the case of configuration NSNS, a slightly larger value of the coupled flux is obtained in any aligned position of the rotor. Nevertheless, it can be stated that both the electromagnetic torque and the main torque do not depend on the phase pole configuration scheme.

The issue looks slightly different in the case of coupled fluxes ψ_{12} and ψ_{13} . In the case of configuration NSNS, significantly higher magnetic coupling occurs between individual phases.

4. Simulations – determination of current and electromagnetic torque instantaneous values

To determine waveforms of the electromagnetic torque and currents in individual phases, a field-circuit model was employed. Calculations were carried out with the following assumptions: supply voltage $U_{dc} = 60 \text{ V}$; turn-on angle $\theta_{\text{on}} = -1.25^\circ$; turn-off angle $\theta_{\text{off}} = 15^\circ$; speed $n = 3000 \text{ rpm}$; winding temperature $T = 70^\circ\text{C}$; full magnetic and electric symmetry of all motor phases. For all configurations depicted in Fig. 1, the electromagnetic torque T_e and phase currents i_{ph} were determined as functions of the rotor position θ . Figures 6 and 7 show plots of the electromagnetic torque T_e as a function of the rotor position θ for configuration NNSS (Fig. 6) in two variants, NNNNNSSSSSS and NSSNNSSNNSSN, and for configuration NSNS (Fig. 7) in variants NNNSSNNSSSS and NSNSNSNSNSNS.

Phase currents i_{ph} as functions of the rotor position θ are shown in Figs. 8 and 9 for configuration NNSS in variants NNNNNSSSSSS and NSSNNSSNNSSN and for configuration NSNS in variants NNNSSNNSSSS and NSNSNSNSNSNS, respectively.

For configuration NNSS in variant NSSNNSSNNSSN and configuration NSNS in variant NSNSNSNSNSNS, the obtained functional dependence of the electromagnetic torque and phase currents on rotor position were very close to each other. At the same time, configuration NSNS is much more sensitive to the scheme of phase placement along the stator magnetic circuit. This is confirmed by values of flux couplings between individual motor phases determined in Section 3 above. At the same time, configuration NNSS is more resistant to the effect of mutual magnetic couplings in the case of variant NNNNNSSSSSS.

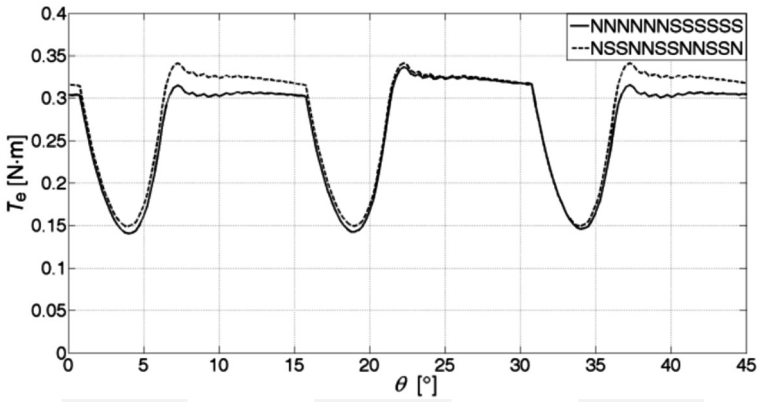


Fig. 6. Electromagnetic torque T_e as a function of the rotor position θ at rotor speed $n = 3000$ rpm for configuration NNSS in two variants

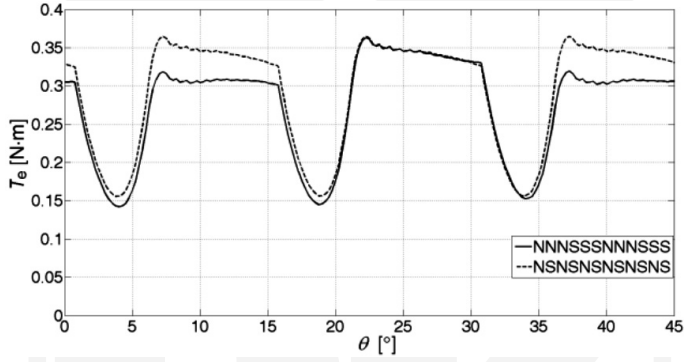


Fig. 7. Electromagnetic torque T_e as a function of the rotor position θ at rotor speed $n = 3000$ rpm for configuration NSNS in two variants

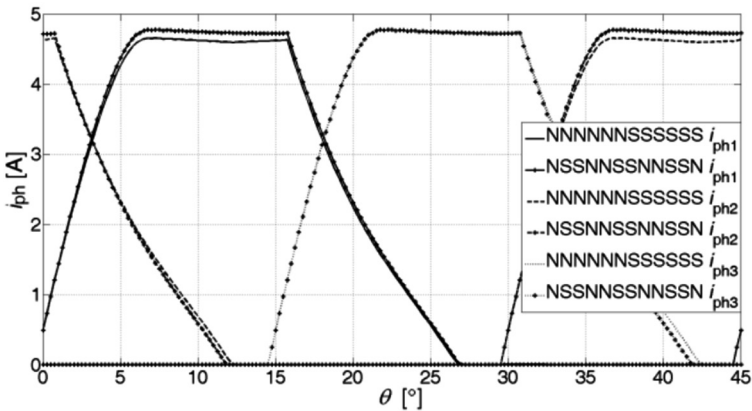


Fig. 8. Phase currents i_{ph} as functions of the rotor position θ at speed $n = 3000$ rpm for configuration NNSS in two variants

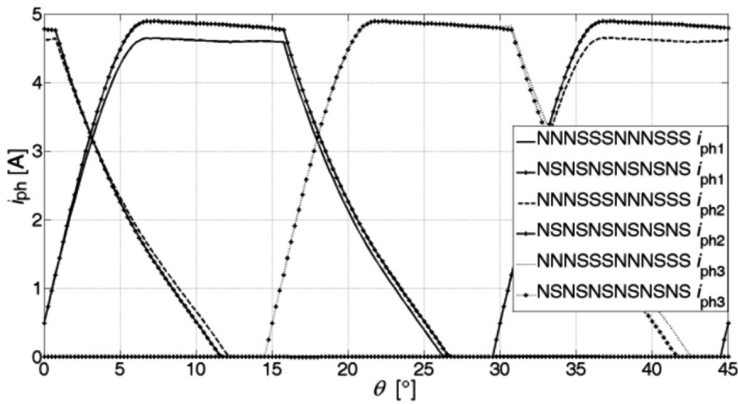


Fig. 9. Phase currents i_{ph} as functions of the rotor position θ at speed $n = 3000$ rpm for configuration NSNS in two variants

5. Laboratory tests

Laboratory tests were carried out in two stages. In the first stage, static characteristics (torque and flux) were determined for both examined configurations. Figure 10 presents a plot of the electromagnetic torque average value T_{eav} as a function of current I for both configurations, i.e. NNSS and NSNS.

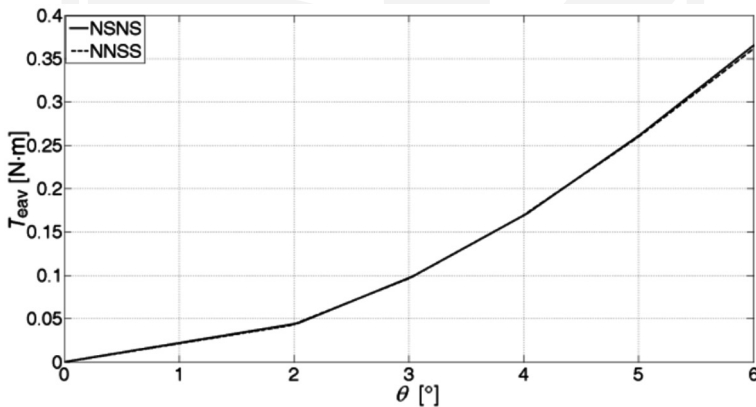


Fig. 10. Electromagnetic torque average value T_{eav} as a function of current I for configurations NNSS and NSNS

As can be observed, the motor torque characteristics obtained in laboratory conditions are almost independent from the configuration type (either NNSS or NSNS). Similar results were obtained on the grounds of the numerical model.

In the second stage of the test, mechanical characteristics of the tested motor were determined and waveforms of its selected parameters were registered. The laboratory setup is shown in Fig. 11.

In view of limitations imposed by the maximum rotation speed of the incremental encoder, the supply voltage value was much lower than the motor's nominal voltage. In the measuring and data acquisition system, the Yokogawa WT1600 six-channel digital power meter equipped with MOTOR module was used. A PC was used for data acquisition and control of the load torque applied to the motor.

At the supply voltage $U_{dc} = 60 \text{ V}$, turn-on angle $\theta_{on} = -1.25^\circ$, and turn-off angle $\theta_{off} = 15^\circ$, mechanical characteristics of the motor were determined for configuration NNSS in variant NNNNNNSSSSSS and configuration NSNS in variant NSNSNSNSNSNS (Fig. 12).



Fig. 11. A view of the laboratory setup

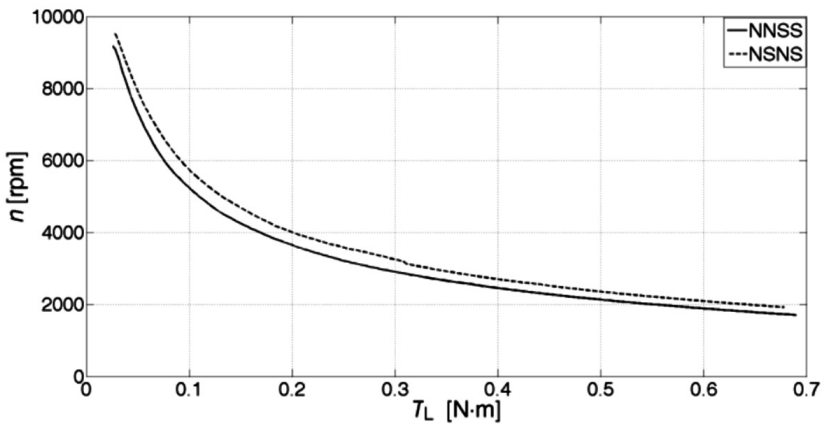


Fig. 12. Rotor speed as a function of load T_L for configurations NNSS (variant NNNNNNSSSSSS) and NSNS (variant NSNSNSNSNSNS)

As can be observed, mechanical characteristics obtained for these two configurations (in selected variants) do not coincide. Configuration NSNS in variant NSNSNSNSNSNS offers higher value of torque on the motor shaft at the same rotor speed with respect to configuration NNSS in variant NNNNNNSSSSSS. This confirms results of simulations obtained earlier for the similar motor operation condition. In an obvious way, this translates into noticeably higher efficiency of the motor than has been observed in laboratory conditions (Fig. 13).

The maximum obtained motor efficiency was 64.5% (at $n = 5057$ rpm) in the case of configuration NNSS and 67% for configuration NSNS (at $n = 5120$ rpm). The registered waveforms of phase currents i_{ph} , the mechanical characteristics of which are presented in Fig. 12, are shown in Fig. 14 (NNSS) and Fig. 15 (NSNS) at the motor speed $n = 3000$ rpm.

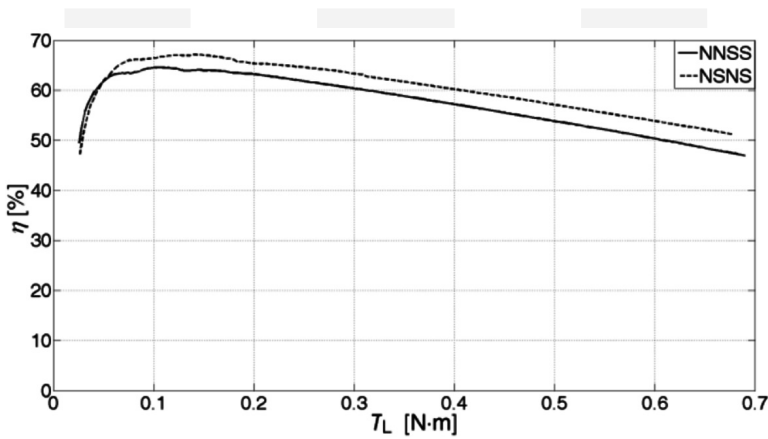


Fig. 13. Motor efficiency as a function of load torque T_L for configurations NNSS (variant NNNNNNSSSSSS) and NSNS (variant NSNSNSNSNSNS)

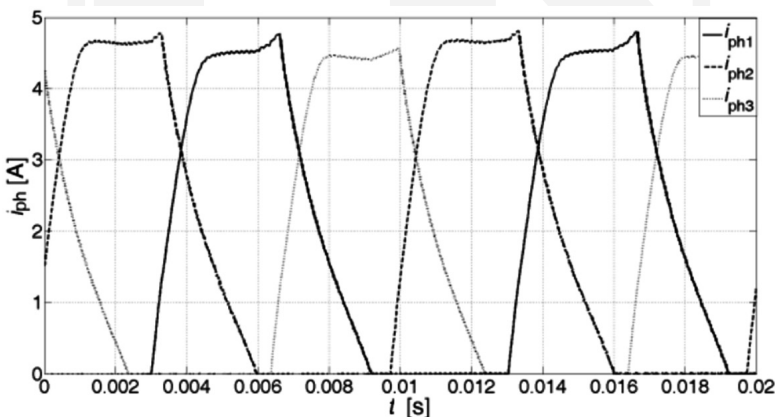


Fig. 14. Phase current waveforms i_{ph} at the motor speed $n = 3000$ rpm for configuration NNSS in variant NNNNNNSSSSSS

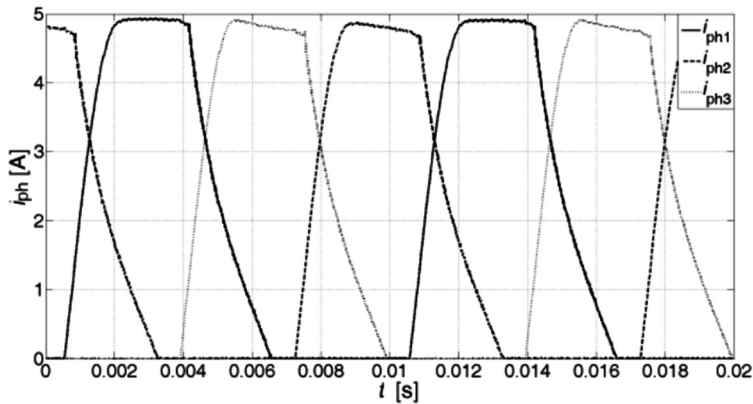


Fig. 15. Phase current waveforms i_{ph} at the motor speed $n = 3000$ rpm for configuration NSNS in variant NSNSNSNSNSNS

In general, the obtained waveforms of currents i_{ph} confirm results obtained from simulations. However, it should be clearly stated that the differences occurring in waveforms of even a single configuration result not only from the presence of magnetic couplings. A quite important effect is in this case related to the magnetic asymmetry that was not taken into account in the simulation model.

6. Summary

In this paper, results of a study on a three-phase 12/8 switched reluctance motor were presented with various configurations of pole winding connections of individual phases. The windings were connected in series in all cases. From the point of view of static characteristics, the pole winding configuration type (either NNSS or NSNS) does not make any practical difference. Both torque characteristics and flux characteristics almost coincide. Fundamental differences occur in values of magnetic fluxes representing couplings between individual phases. The configuration of NNSS type is characterized by values of magnetic couplings that are several times lower. Simulations performed with the use of a field-circuit model proved that configuration NSNS is more susceptible to the effect of magnetic couplings. This is noticeable especially in the case where, for example, the NNNSSNNSS variant was used. Configuration NNSS is less susceptible to the effect of magnetic couplings. At the same time, in the case of the NNSS configuration, slightly lower values of phase currents and the produced electromagnetic torque were obtained. Laboratory tests confirmed results of simulations in scope of both static characteristics and phase current waveforms. Undoubtedly, the most favourable case is configuration NSNS in the NSNSNSNSNSNS variant. However, only slightly worse results were obtained in the case of the NNSS configuration in variant NSSNNSSNNSSN. Phase current waveform patterns are influenced not only by magnetic couplings from neighbouring phases but also by the way in which the phases are arranged with respect to each other. Moreover, laboratory tests revealed quite a significant effect of magnetic asymmetry between individual phases. This phenomenon is clearly visible in Figs. 14 and 15.

References

- [1] Miller T.J.E., *Faults and unbalanced force in the switched reluctance machine*, IEEE on Industry Applications, 1995, Vol. 31(2), pp. 319–328.
- [2] Ferreira C.A., Jones S.R., Heglund W.S., Jones W.D., *Detailed design of a 30-kW switched reluctance starter/generator system for a gas turbine engine application*, IEEE Trans. Ind. Appl., 1995, Vol. 31(3), pp. 553–561.
- [3] Pochanke A., *Modele obwodowo-polowe pośrednio sprzężone silników bezzestykowych z uwarunkowaniami zasilania. Monografia [Indirectly coupled circuit-field models for brushless motors with conditioned supply. A monograph]*, Oficyna Wydawnicza Politechniki Warszawskiej, Warszawa 1999.
- [4] Miller T.J.E., *Electronic control of switched reluctance machines*, Newnes, 2001.
- [5] Li J., Sun H., *Modeling and simulations of four-phase 8/6 switched reluctance motor with an improved winding configuration*, International Conference on Computer Science and Software Engineering, 2008, Vol. 4, pp. 1045–1048.
- [6] Bogusz P., Korkosz M., Prokop J., *Wyznaczanie charakterystyk statycznych maszyn reluktancyjnych przelączalnych [Determination of static characteristics of switched reluctance machines]*, Zeszyty Problemowe — Maszyny Elektryczne, 2005, No. 72, pp. 53–58.
- [7] *Flux 11.1 Documentation*, 2012, Cedrat Group.

